
Trans-typology design space exploration: Using gradients to inform decision-making in the design of spanning structures

Demi FANG^{*a}, Peter WANG^b, Sophia V. KUHN^c, Michael A. KRAUS^d, Caitlin MUELLER^a

^{*a}Massachusetts Institute of Technology
77 Massachusetts Ave Room 5-418, Cambridge, MA 02139, USA
dfang@mit.edu

^b HNTB
^c ETH Zurich
^d TU Darmstadt

Abstract

Structural designers pursuing high-performance design must typically make decisions based on perceived tradeoffs. As an alternative to the extreme paradigms of deploying rules of thumb and blackbox optimization, a new paradigm of “performance-informed, human-driven design” is proposed in which designers extract data-driven insights from a provided design space to inform decision-making. The four-step computational framework entails selecting a sample representative of the design space of interest, training a machine learning model, computing gradients of the model, and computing influence metrics. Applied to the case study of a long-span structure, this paper demonstrates how this gradient-based approach can offer a data-driven way to support and augment intuitions about performance-driven design. Choice of structural typology is demonstrated to be most associated with large changes of GWP. As designers make decisions that refine the design space of interest, the framework can be iteratively applied at neighborhoods of the original design space, here revealing how priorities of other decisions (span, live load, embodied carbon coefficient) vary by typology. This case study application showcases how decision-making insights tailored to specific problems can be derived from intricate mixed-variable design domains, underscoring the potency of such approaches in informing system-level design processes for low-carbon structures.

Keywords: design space exploration, gradients, computational design, parametric design, embodied carbon, long-span structures, conceptual structural design, sensitivity analysis, generative AI

1. Introduction

Does a timber beam or a steel truss result in a lighter structure? Between shortening the span and decreasing the load demand, which results in a more efficient structure? Structural designers pursuing high-performance design must typically make decisions based on perceived tradeoffs. To address these complex decision-making processes, designers can typically choose among a few paradigms, such as optimization and deploying rules of thumb. Optimization delivers design solutions from a blackbox without conveying information about the design problem (“the lightest design is made of timber”). Deploying rules of thumb is a way for designers to implement intuition based on general design experience (“using timber usually results in lower embodied carbon”), but it is less quantitatively informed for specific design problems where generalized rules of thumb may not apply everywhere in the design space. Moreover, it is not intuitive to quantitatively compare the effects of design decisions and evaluate trade-offs within these existing paradigms (“How does shortening the span of the concrete beam compare to using timber instead?”).

A new paradigm of performance-driven structural design is proposed where designers are empowered to make quantitatively informed decisions based on data from the design space of the specific design problem at hand. This framework is made possible by a four-step computational procedure, initially proposed in [1]. Applied here to the case study of a long-span structure, it is now possible to answer the example questions posed above: performance data of specific design spaces can be leveraged to quantitatively confirm or supplement intuition and rules of thumb. Performance trade-offs that were previously un-intuitive, such as choice of material against span, are made comparable through this framework. The approach also balances specific insights from local neighborhoods of the design space against general insights from the global design space, while contributing to validation and augmentation of “rules of thumb” at a global level of design. The results demonstrate a paradigm shift from “performance-driven design” to “performance-informed, human-driven design.”

2. Background and literature

Many methods are available to optimize and explore continuous design spaces, or design spaces where all variables are numerical. Gradients are key in these methods: they measure change in performance relative to change in each continuous variable. Gradients are mathematically defined and readily available; their computation via finite differencing [2] or automatic differentiation of machine learning models [3] have been demonstrated for applications of design space exploration. In contrast, design space exploration methods are limited in mixed-variable design spaces, or design spaces that contain both continuous variables and discrete variables (choices between discrete values, such as structural material). Optimization methods such as mixed integer programming exist for optimizing in mixed-variable design spaces, but there are limited methods for navigating through them.

A framework for computing “influence metrics” in mixed variable design spaces was first proposed in [1], establishing a way to define and compare “gradients” across continuous and categorical variables. While [1] applies the framework to the design of gridshells, in this paper, the framework is applied to a high-impact design problem of designing a low-carbon long-span structure, demonstrating the framework’s ability to augment intuition in the complex design spaces of low-carbon structural design.

3. Methodology

3.1 Framework for computing influence

An overview of the method specific to low-carbon structural design is described in this section and in Figure 1. The first step of generating design data is key for the designer to communicate the extents of the design space. The data include the design variables and a single performance objective. More details on the conditional variational autoencoder (cVAE) are available in [3] and on the computing influence metrics in [1], [4].

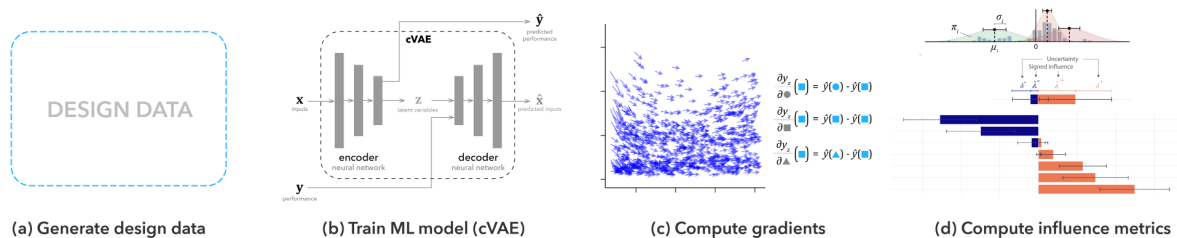


Figure 1: Four-step methodology for determining influence metrics from a given design space.

Gradients are mathematically defined for continuous variables, but not for categorical variables. In this framework, a definition for “gradients” of performance relative to each category of a categorical variable is proposed as the difference in performance between a reference design and the same design with the categorical variable switched to the category of interest (Figure 2) [4]. These gradients are comparable across continuous and discrete variables due to variable pre-processing; the distributions of continuous variables are standardized (i.e. their pre-processed distribution has a mean of 0 and standard deviation of 1), while categorical variables are one-hot-encoded (Figure 3). As a result, one unit of change is

associated with a) 1 standard deviation of a continuous variable's distribution in the design space and b) 1 change of category for categorical variables (Figure 4). Performance is also standardized (Figure 3), meaning the gradients are unitless.

example:
given a design \blacksquare and
 $x_{b,i} \in \{ \bullet, \blacksquare, \blacktriangle \}$,
the gradients for each category are:

$$\frac{\partial y_z}{\partial \bullet} (\blacksquare) = \hat{y}(\bullet) - \hat{y}(\blacksquare)$$

$$\frac{\partial y_z}{\partial \blacksquare} (\blacksquare) = \hat{y}(\blacksquare) - \hat{y}(\blacksquare)$$

$$\frac{\partial y_z}{\partial \blacktriangle} (\blacksquare) = \hat{y}(\blacktriangle) - \hat{y}(\blacksquare)$$

Figure 2: Example definition of gradients for a categorical variable's categories.

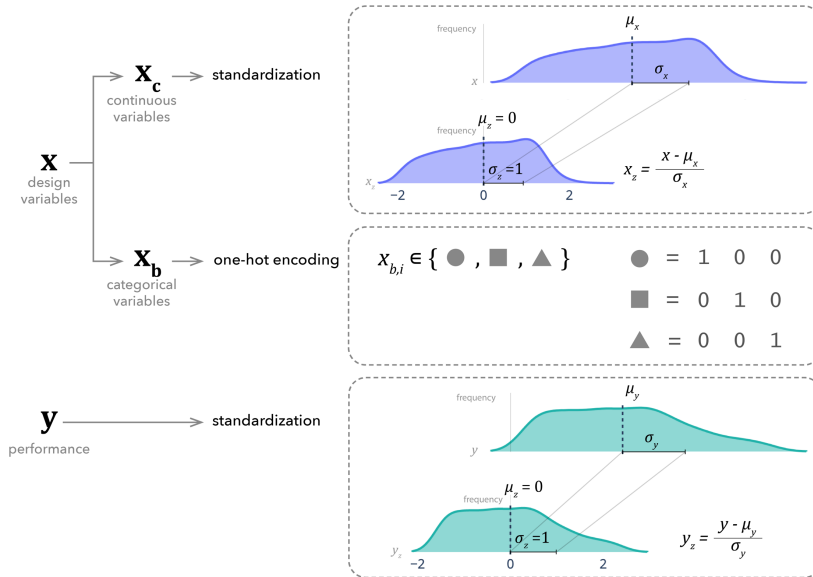


Figure 3: Pre-processing of variables and performance objective before cVAE training.

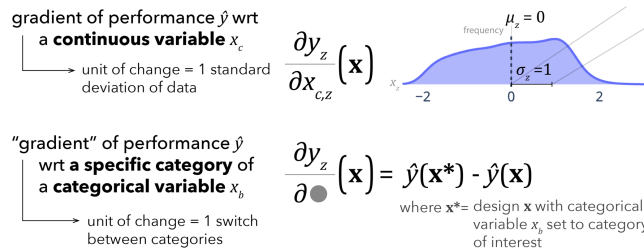


Figure 4: Comparability of gradients with respect to continuous variables, and "gradients" with respect to categories of categorical variables.

3.2 Long-span design problem

The long-span design problem used as a case study application of this framework is inspired by the Kimbell Art Museum by Louis Kahn and August Komendant (1972) and its extension by Renzo Piano Building Workshop (2013). The former features a concrete barrel beam spanning 30 m, and the latter spans similar modules with a different typology: pairs of glulam beams. How does global warming potential (GWP) intensity change with choice of spanning typology relative to other design decisions?

This question guiding decision-making in early-stage design can be addressed by applying the framework introduced in 3.1. For the design data, a variety of structural typologies are designed to support a long-span roof (Figure 5): steel and timber girders and trusses, and an elliptical barrel beam of reinforced concrete (a simplified version of the original cycloid-shaped barrel beam, which was pre-stressed).

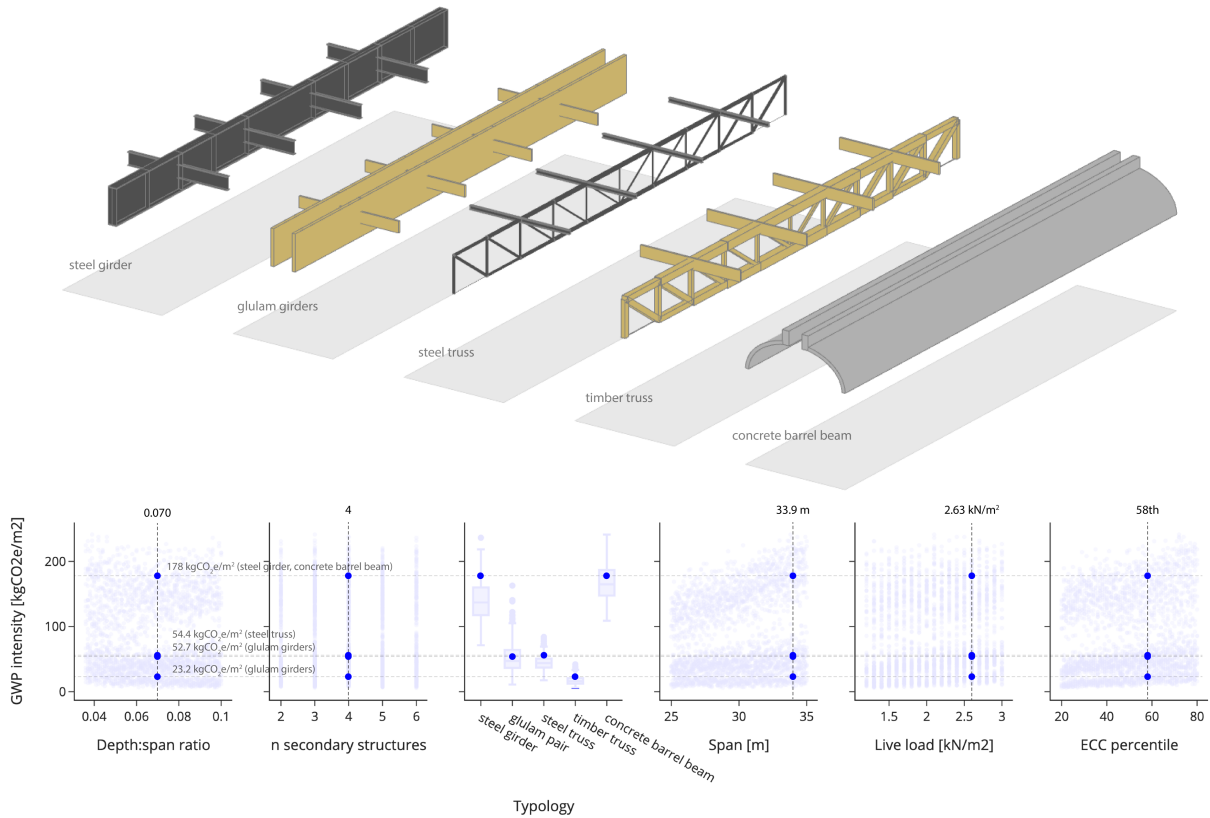


Figure 5: Five long-span typologies designed for a long-span roof design problem and the position of the depicted parameters in the design space. A visual sampling of the design space is available in the Appendix.

This design space and assumptions mock up an early-stage exploration of a long-span design problem. A bottom-up parametric structural model is developed to generate the design space by taking design variables and computing GWP intensity using material quantities and embodied carbon coefficients (ECCs); details on this model are provided in Table 1. Each structural typology has a different design approach, which are detailed in Table 2. Finally, material assumptions are presented in Table 3.

Table 1: Design parameters and constraints for generating the parametric dataset representing the design space.

Design variables	Depth:span ratio: [0.036 to 0.100] Number of secondary structures: [2 to 6] Typology: {steel built-up girder, glulam pair of beams, steel round-tube truss, timber square-section truss, reinforced concrete elliptical barrel beam} Span: [25.0 to 35.0 m] Live load: [1.2 to 3.0 kN/m ²] Embodied carbon coefficient (ECC) percentile: [20, 80] (see Table 3)
Other constraints	Tributary width: 7 m
Performance objective	GWP intensity, or $\frac{GWP}{\text{roof area}}$, where roof area = span \times tributary width = $L \times 7$ m, and $GWP = \sum SMQ \times ECC$, where SMQ = structural material quantities (kg) and ECC = embodied carbon coefficient of the material (kg CO ₂ e/kg) [5] A1-A3 ECCs are used, and ranges are detailed in Table 3.

Design space sampling technique	Latin Hypercube sampling, 500 designs per typology (2500 total designs)
Load cases and combinations	<ul style="list-style-type: none"> • Distributed dead load DL (by weight; for magnitudes see Appendix) • Distributed live load LL (for magnitudes see Design variables in Table 1) • LL_{asym}: distributed live load applied on half of the primary span • DL+LL • DL+LL_{asym}
Engineering assumptions	<p><i>Strength</i>: maximum utilization of 70% for DL+LL and DL+LL_{asym} <i>Serviceability</i>: Maximum displacement of $L/360$ under LL Trusses: strength and serviceability uniquely enforced; see Table 2. Sections are automatically sized to the smallest section in a provided series meeting the engineering design criteria (using Karamba’s Optimize Cross-section component [6]). Connection quantities are not included.</p>

Table 2: Design approach for each structural typology based on design variable of structural depth. Each structural material is assumed to have a single grade, detailed in Table 3.

Structural typology: primary system	Design approach based on master design variable of structural depth, d
Steel girder	<p>Minimum dimensions of the built-up plate girder are selected based on rules of thumb [7]. The minimum weight girder section from sections exceeding these minima:</p> <ul style="list-style-type: none"> • Minimum web thickness $t_w = d/150$, pick from series incremented 0.5 cm above the minimum • Minimum flange thickness $t_f = 1.1t_w$, pick from series incremented 0.5 cm above the minimum • Minimum flange width $b_f = d/6$, pick from series incremented 1 cm above the minimum <p>Placement and design of transverse stiffeners on the plate girder:</p> <ul style="list-style-type: none"> • Transverse stiffeners are placed everywhere a secondary member frames into the girder • If the spacing of secondary members exceeds $2d$, at the outer quarters of the primary span (from each end to $L/4$), the minimum number of additional stiffeners are placed evenly between secondary members at a maximum spacing of $2d$ • Stiffener thickness is designed based on required moment of inertia of the stiffener, I_{st}, per AISC [8] Section G2.2 <p>Secondary system:</p> <ul style="list-style-type: none"> • Select minimum weight from typical American W-section series, enforcing a minimum depth of $d/3$ <p>Deflection under live load calculated from structural analysis model</p>
Pair of glulam girders	<p>Dimensioning the width of the glulam girders:</p> <ul style="list-style-type: none"> • Solve for minimum width of an individual girder based on d and slenderness ratio (R_B) limit of 50 (NDS [9] 3.3.3.6) • For the analysis model, a single girder was modeled, with a minimum width of twice the minimum width calculated above for an individual glulam girder • Assume the glulam beams within the pair are spaced 1.5 m apart for higher moment of inertia against lateral buckling <p>Secondary system: softwood timber beams with depth-to-width ratio of 6 Assume additional 10% GWP for the steel needed to activate composite action between the girders (see Renzo Piano Building Workshop’s Kimbell Art Museum Expansion for a built example) Deflection under live load calculated from structural analysis model</p>
Steel truss	<p>2 panels between each secondary member Cross-sections: hollow tube with diameter-to-thickness ratio of 20 Secondary system: select minimum weight from typical American W-section series Maximum utilization of 35% (determined empirically) applied in lieu of enforcing deflection constraint</p>
Timber truss	<p>2 panels between each secondary member Cross-sections: solid square softwood Secondary system: same as for glulam beam pair Maximum utilization of 30% (determined empirically) applied in lieu of enforcing deflection constraint</p>
Reinforced concrete barrel beam	<p>Elliptical barrel geometry created by stretching a semicircular arc with radius d to fit the tributary width The light well gap at the top of the arc is defined as a 30-degree sector Calculating thickness t of the barrel beam:</p> <ul style="list-style-type: none"> • Maximum moment M_{max} calculated under DL+LL and DL+LL_{asym}, assuming 15 cm thickness for initial DL estimate • Minimum required area of concrete “ribs” at top of beam, $A_{min,c}$, dimensioned to carry compression of $M_{max}/0.75d$ ($0.75d$ approximates a reduction of the inner lever arm due to placement of required steel from bottom of section) • Each curb in the pair is assumed to have depth of $4t$ and width of $2t$. Solve for t given $A_{min,c}$ and $A_{total}=16t^2$ <p>Reinforcing by volume for material quantities and GWP calculation: larger of {required area of steel as proportion of full cross-section; 2% by volume} No secondary system needed; “number of secondary structures” design variable is not applicable Deflection under live load calculated from structural analysis model of an equivalent semi-elliptical shell with a concrete material that had a tension strength equal to its compressive strength</p>

Table 3: 20th and 80th percentile embodied carbon coefficients of materials as converted from [10]. See Appendix for reference values in their original units and other material values (specific weight, strength, stiffness).

Material	Typology and elements	Embodied Carbon Coefficient (A1-A3) [kg CO ₂ e/kg]	
		20 th percentile	80 th percentile
Steel plate	Steel girder (primary system)	1.55 kg CO ₂ e / kg	1.65 kg CO ₂ e / kg
Steel hot-rolled section	Steel girder (secondary system)	0.650 kg CO ₂ e / kg	0.850 kg CO ₂ e / kg
Steel hollow section	Steel truss (secondary system)	1.40 kg CO ₂ e / kg	1.70 kg CO ₂ e / kg
Glue-laminated timber	Pair of glulam girders (primary)	0.275 kg CO ₂ e / kg	0.628 kg CO ₂ e / kg
Softwood timber (ECCs of glulam by volume used conservatively)	Pair of glulam girders (secondary)	0.392 kg CO ₂ e / kg	0.897 kg CO ₂ e / kg
Ready-mix concrete, 27.6 MPa (4000 psi) normal weight	Timber truss (primary and secondary)	0.121 kg CO ₂ e / kg	0.176 kg CO ₂ e / kg
Rebar, fabricated	Reinforced concrete barrel beam (partial by volume, see Table 2)	0.739 kg CO ₂ e / kg	0.925 kg CO ₂ e / kg

4. Results and discussion

4.1 Exploratory data analysis (EDA)

Plotting the performance metric of GWP intensity against each design variable of interest is a typical exploratory data analysis (EDA) technique done as a first pass at understanding the scope of the design space (Figure 6). Each plot offers a projected view of the multi-dimensional design space, and a few limited trends between GWP intensity and each variable can be observed. For example, while there are large differences in GWP intensity between different typologies, each typology shows large enough variations in GWP intensity (due to the high dimensionality of other variables) that there are overlaps: some concrete barrel beams have similar performance to glulam girder designs. Other slight trends such as an increase of GWP intensity with span, live load, and ECC percentile are evident as expected, while the relationship between GWP intensity and depth is complex and varies across different typologies. These limited insights in the high-dimensional mixed-variable design space motivate the computation of influence metrics for this dataset.

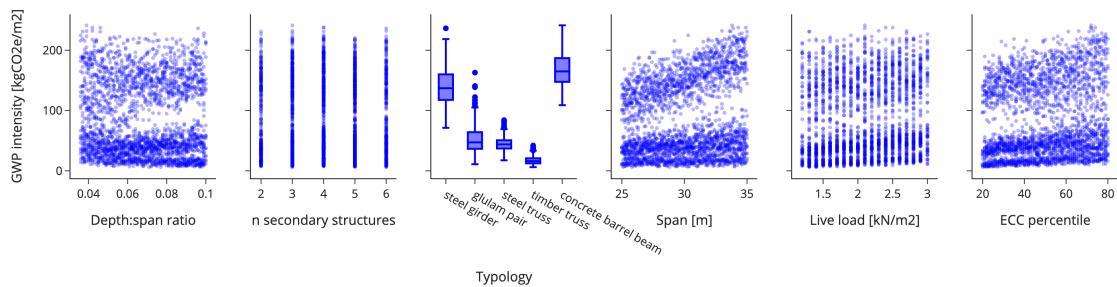


Figure 6: GWP intensity vs. design variables in the provided design space.

4.2 Machine learning training

A variant of the cVAE deployed in [3] was trained on the design data. Layer widths of [64, 32] were used for both the encoder and decoder, resulting in an acceptable R^2 value of 0.987 in predicted vs. true GWP intensity values on test data not seen during training, with a root mean-squared error of 7.1 kg CO₂e/m².

4.3 Influence metrics

For more details on how each type of influence metric is computed, the reader is referred to the framework as introduced in [1]. The influence metrics in Figure 7 are appropriate for high-level design decision-making: of the design variables and ranges provided in the original design space, GWP

intensity changes the most with choice of typology, though with large variance across the design space (large whisker on the influence bar).

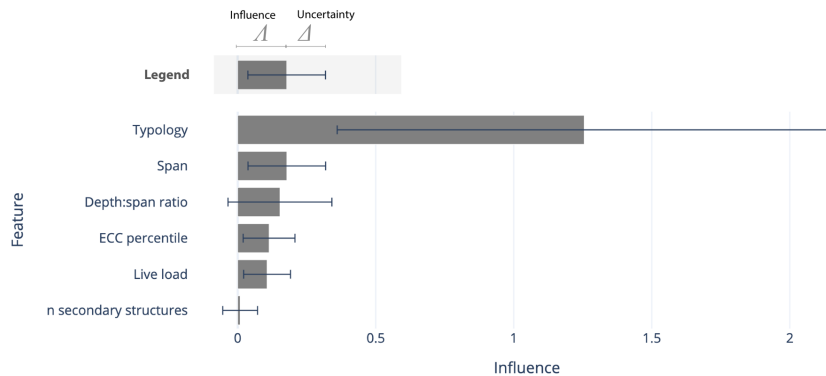


Figure 7: Overall influence metrics of design features on GWP intensity.

For finer level of insights, signed influence metrics are useful (Figure 8). Selecting the timber truss is the decision found to be most associated with large reductions in GWP intensity, followed closely by the steel truss and the glulam pair. Selecting the concrete barrel beam is shown to be most associated with large increases in GWP intensity, followed moderately by selecting a steel girder. Choice of typology are decisions that dominate the extremes of signed influence. It is significant to be able to compare categorical against continuous variables within this framework. For example, the association of an increase in ECC percentile with very moderate increases in GWP intensity relative to selection of typology suggests that in this design space, the relative uncertainty of ECCs during early-stage design is not a hindrance: even if the full range of 20th to 80th percentiles of ECCs are considered, none are as influential on GWP as choice of typology. Similar conclusions can be made about choice of typology against the other continuous variables of span, structural depth, live load, and number of secondary structures. These insights are intentionally to be interpreted within the context of this design space, i.e. they are only applicable for the ranges of variables provided in the design dataset.

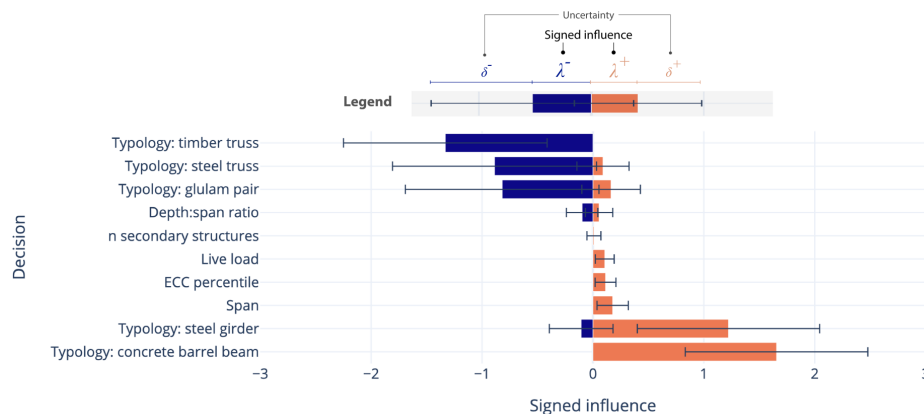


Figure 8: Signed influence metrics of design decisions on GWP intensity. Large dark-blue bars indicate a large association with reductions in GWP intensity, and orange with increases. For continuous variable decisions, the sign of influence is associated with an increase in the continuous variable.

4.4 Constricting or expanding the design space to inform decision-making at any stage of design

What happens after influence metrics inform a decision? An advantage of the methodology as outlined in Figure 1 is that the designer has full control over the scope of insights by expanding or constricting the design space through the first step of provided design data. As an example, a designer might read Figure 8 and decide to eliminate steel girders and concrete barrel beams from the design space given their high influence on GWP increases. This neighborhood of the design space can be substituted into step 1 of Figure 1 to clarify which of the remaining decisions to prioritize. The updated signed influence

metrics (Figure 9) communicate that for the smaller design space under consideration, choosing the glulam girders can be a worse choice for GWP intensity than increasing span, live load, or ECC percentile. This is also often, but not always, true for choosing the steel truss.

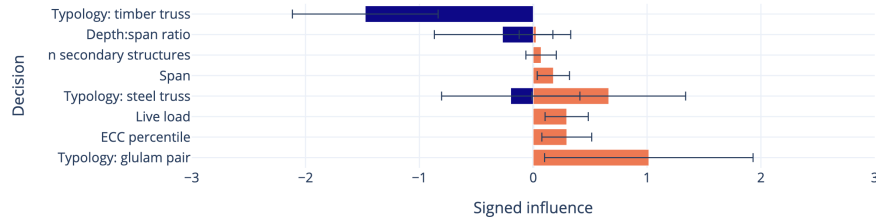


Figure 9: Signed influence metrics of design decisions on GWP intensity after removing the steel girder and concrete barrel beam from the design data.

Another possible design scenario or iteration is that the designer decides on a particular typology and wants to understand the resulting priorities for this smaller neighborhood of designs. The resulting influence metrics of three possible typologies are shown in Figure 10. The differences in priorities among the three different typologies highlights how more tailored decision-making recommendations can be produced after narrowing the initially diverse design space. For example, Figure 10 (b) suggests that the designer who chooses a steel truss might be most concerned with the sensitivity of those designs' GWP to live load; this makes sense intuitively because the steel truss has a low dead load compared to the other typologies, and live load would govern its material quantities. The designer who chooses to make decisions on a glulam girder (Figure 10 (a)) need not worry as much about span as the designer who chooses to make decisions on a concrete barrel beam (Figure 10 (c)).

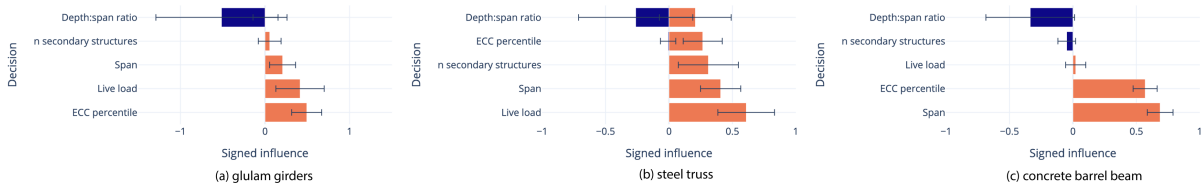


Figure 10: Signed influence metrics of design decisions on GWP intensity for the local neighborhood of each of three typologies: (a) glulam girders, (b) steel truss, (c) concrete barrel beam.

Note that magnitudes of influence are mainly for comparative purposes within a design space and might not be comparable across different design spaces. For more details, the reader is referred to [1], [4].

5. Limitations

5.1 Limitations in the parametric structural model of this case study

In this model, A1-A3 embodied carbon coefficients are used, meaning that construction emissions are not reflected in GWP estimates. Construction stage emissions would differ greatly by structural typology: for example, the concrete barrel beam may require more emissions to construct due to the large amount of formwork. Connection quantities were also omitted but may introduce a premium on quantities for girder and truss typologies. Design rules for secondary members could also be further refined, but the focus in scope of this early-stage structural design example was on the typology of the primary member. The concrete beam typology includes roof-area spanning material, which gives it slightly higher material quantities than the other typologies. Including roof-area spanning material for the other typologies would affect the influence of “number of secondary structures” on GWP intensity due to the variable’s influence on the depth of spanning material. Finally, some materials such as concrete are known to exhibit a relationship between strength and embodied carbon coefficients. In this study, a range of ECC values were allowed, but material grades were kept uniform. Accounting for interpolations between material strength and ECC (such as those provided in [10]) could improve estimates in material, and GWP, efficiency.

5.2 Limitations in the framework of computing influence metrics

Of the steps in the framework outlined in Figure 1, the first step of producing a parametric model to generate synthetic data is the most time-consuming. (While possible to apply the framework on “wild” data of emissions measured from the industry, these data are typically not yet at suitable quality and quantity for meaningful machine learning.) It takes time and expertise for designers to set up a parametric model and design parameters that cover the design space of interest, and this process is often iterative.

One particular challenge in this process, regardless of field expertise, is developing the parametric model such that the design variables of the parametric design space drive an aspect of every structural typology. With different enough structural typologies and associated design approaches, it may get more and more difficult to identify parameters that are shared among typologies. For example, in this design example, the “ECC percentile” design variable was necessary to drive the ECC values of different materials used across different typologies. It was not possible to be typology-agnostic with every design variable: in this example, “number of secondary structures” was applicable to every typology except the reinforced concrete barrel beam.

Despite these challenges in developing the parametric model to generate design data, once the parametric framework was finalized, the generation of 2500 designs for this design problem took 30-40 minutes, and the training of the machine learning and the computation of gradients and influence metrics took even less time (on the order of 60 seconds). The ultimate payoff of being able to compare decisions through the influence metrics is significant. There are also beneficial scenarios in which such parametric models and their trained models could be developed for often-used structural systems and be reused for multiple projects.

6. Conclusion

A framework for comparing change in performance relative to both continuous and categorical design variables is applied to a high-impact structural design problem of a low-carbon long-span roof. Designers typically make decisions during early-stage design based on experience and intuition, but this framework offers a way to validate and augment those intuitions in a data-driven way. For example, designers might have some intuition around a concrete beam being a heavier system and trusses being more materially efficient, but might not necessarily understand the magnitude with which those differences in material efficiency might relate to GWP intensity compared to changes in live load, span, or embodied carbon coefficients. The influence metrics produced by this approach (Figure 7, Figure 8) provide a data-driven and accessible snapshot (compared to high-dimensional EDA) for supplementing those intuitions.

Applying this framework to other synthetic datasets of structural design can help clarify which decisions are worth taking in complex design spaces. Quality synthetic datasets of embodied carbon in structural systems are becoming more prevalent in the literature and in practice, such as multi-story structural systems with foundations [11], [12] and mass timber structural systems [13], [14], [15]. Leveraging these data are a key strategy for pursuing low-carbon design [16], both in developing a greater understanding of rules of thumb and in informing decision-making for specific design problems.

Any performance-driven design problem must grapple with a balance of rules of thumb based on general intuition and recommendations based on the specificity of the design problem at hand. Data in such performance-driven design problems, such as low-carbon structural design, can be leveraged to help inform the latter approach of specificity. These findings demonstrate how this data can be utilized to effectively support these complex decision-making processes, empowering a paradigm of performance-informed, human-driven design.

Acknowledgements

The idea of comparing spanning alternatives of the Kimbell originates from Prof. John Ochsendorf in the beam analysis unit of his curriculum for “Introduction to Structural Design” at MIT Departments of Architecture and Civil Engineering. Demi Fang was supported by the J. A. Curtis (1953) Fund from MIT School of Architecture + Planning.

References

- [1] D. Fang, S. V. Kuhn, W. Kaufmann, M. A. Kraus, and C. Mueller, “Quantifying the influence of continuous and discrete design decisions using sensitivities,” in *Advances in Architectural Geometry 2023*, Stuttgart, Germany, Oct. 2023. doi: 10.1515/978311162683-031.
- [2] N. C. Brown and C. T. Mueller, “Gradient-based guidance for controlling performance in early design exploration,” in *Proceedings of the International Association for Shell and Spatial Structures (IASS) Symposium*, Boston, MA, 2018.
- [3] V. M. Balmer and S. V. Kuhn *et al.*, “Design Space Exploration and Explanation via Conditional Variational Autoencoders in Meta-model-based Conceptual Design of Pedestrian Bridges.” arXiv, Nov. 29, 2022. doi: 10.48550/arXiv.2211.16406.
- [4] D. Fang, “System-level design of low-carbon structures,” PhD, Massachusetts Institute of Technology, Cambridge, MA, USA, 2024.
- [5] C. De Wolf, F. Yang, D. Cox, A. Charlson, A. S. Hattan, and J. Ochsendorf, “Material quantities and embodied carbon dioxide in structures,” *Proceedings of the Institution of Civil Engineers - Engineering Sustainability*, Sep. 2015, doi: 10/gg55mf.
- [6] C. Presinger and Bollinger+Grohmann, “Karamba.” 2018. [Windows]. Available: <http://www.karamba3d.com/>
- [7] National Steel Bridge Alliance, “Design Example 1: Three-span continuous straight composite steel I-girder bridge,” in *Steel Bridge Design Handbook Appendix*, American Institute of Steel Construction, 2022. [Online]. Available: https://www.aisc.org/globalassets/nsba/design-resources/steel-bridge-design-handbook/b951_sbdh_appendix1.pdf
- [8] American Institute of Steel Construction, *Steel Construction Manual*, 14th ed. American Institute of Steel Construction, 2011.
- [9] American Wood Council, *National Design Specification for Wood Construction, 2018 edition*. American Wood Council, 2017. [Online]. Available: <http://www.awc.org/codes-standards/publications/nds-2018>
- [10] Carbon Leadership Forum, “2023 Carbon Leadership Forum: North American Material Baselines, Category Appendices v2,” Aug. 2023. [Online]. Available: <https://carbonleadershipforum.org/clf-material-baselines-2023/>
- [11] P. Foraboschi, M. Mercanzin, and D. Trabucco, “Sustainable structural design of tall buildings based on embodied energy,” *Energy and Buildings*, vol. 68, no. Part A, pp. 254–269, Jan. 2014, doi: 10/f5pzn8.
- [12] H. L. Gauch, W. Hawkins, T. Ibell, J. M. Allwood, and C. F. Dunant, “Carbon vs. cost option mapping: A tool for improving early-stage design decisions,” *Automation in Construction*, vol. 136, p. 104178, Apr. 2022, doi: 10.1016/j.autcon.2022.104178.
- [13] I. Hens, R. Solnosky, and N. C. Brown, “Design space exploration for comparing embodied carbon in tall timber structural systems,” *Energy and Buildings*, vol. 244, p. 110983, Aug. 2021, doi: 10.1016/j.enbuild.2021.110983.
- [14] S. J. Leonard and R. Solnosky, “Guiding Mass Timber Design and Research: A Parametric Modeling Approach to Understanding Impacts,” pp. 230–246, May 2023, doi: 10.1061/9780784484777.021.
- [15] S. Leonard, N. C. Brown, and R. Solnosky, “Impact of Prescriptive Fire Design Provisions on Embodied Carbon for International Building Code Type IV Construction,” *Practice Periodical on Structural Design and Construction*, vol. 29, no. 2, p. 04024012, May 2024, doi: 10.1061/PPSCFX.SCENG-1418.
- [16] D. Fang, N. Brown, C. De Wolf, and C. Mueller, “Reducing embodied carbon in structural systems: A review of early-stage design strategies,” *Journal of Building Engineering*, vol. 76, p. 107054, Oct. 2023, doi: 10.1016/j.job.2023.107054.

Appendix

A digital appendix is provided online at: <https://demifang.github.io/spanning-typs-2024>